SPECIAL ISSUE ARTICLE

Mechanical crosstalk between the intervertebral disc, facet joints, and vertebral endplate following acute disc injury in a rabbit model

Matthew Fainor[1,2] | Brianna S. Orozco[1,2] | Victoria G. Muir[3] |
Sonal Mahindroo[2,4] | Sachin Gupta[1,2] | Robert L. Mauck[1,2,3] |
Jason A. Burdick[3,5] | Harvey E. Smith[1,2] | Sarah E. Gullbrand[1,2]

[1]Department of Orthopaedic Surgery, McKay Orthopaedic Research Laboratory, Perelman School of Medicine, University of Pennsylvania, Philadelphia, Pennsylvania, USA

[2]Translational Musculoskeletal Research Center, Corporal Michael J. Crescenz VA Medical Center, Philadelphia, Pennsylvania, USA

[3]Department of Bioengineering, University of Pennsylvania, Philadelphia, Pennsylvania, USA

[4]Department of Biology, St. Bonaventure University, St. Bonaventure, New York, USA

[5]BioFrontiers Institute and Department of Chemical and Biological Engineering, University of Colorado Boulder, Boulder, Colorado, USA

Correspondence
Sarah E. Gullbrand, Department of Orthopaedic Surgery, McKay Orthopaedic Research Laboratory, Perelman School of Medicine, University of Pennsylvania, Philadelphia, PA, USA.
Email: sgullb@pennmedicine.upenn.edu

Abstract

Background: Vertebral endplate sclerosis and facet osteoarthritis have been documented in animals and humans. However, it is unclear how these adjacent pathologies engage in crosstalk with the intervertebral disc. This study sought to elucidate this crosstalk by assessing each compartment individually in response to acute disc injury.

Methods: Eleven New Zealand White rabbits underwent annular disc puncture using a 16G or 21G needle. At 4 and 10 weeks, individual compartments of the motion segment were analyzed. Discs underwent T_1 relaxation mapping with MRI contrast agent gadodiamide as well T_2 mapping. Both discs and facets underwent mechanical testing via vertebra—disc—vertebra tension-compression creep testing and indentation testing, respectively. Endplate bone density was quantified via μCT. Discs and facets were sectioned and stained for histology scoring.

Results: Intervertebral discs became more degenerative with increasing needle diameter and time post-puncture. Bone density also increased in endplates adjacent to both 21G and 16G punctured discs leading to reduced gadodiamide transport at 10 weeks. The facet joints, however, did not follow this same trend. Facets adjacent to 16G punctured discs were less degenerative than facets adjacent to 21G punctured discs at 10 weeks. 16G facets were more degenerative at 4 weeks than at 10, suggesting the cartilage had recovered. The formation of severe disc osteophytes in 16G punctured discs between 4 and 10 weeks likely offloaded the facet cartilage, leading to the recovery observed.

Conclusions: Overall, this study supports that degeneration spans the whole spinal motion segment following disc injury. Vertebral endplate thickening occurred in response to disc injury, which limited the diffusion of small molecules into the disc.

Matthew Fainor and Brianna S. Orozco contributed equally to this study.

This work also suggests that altered disc mechanics can induce facet degeneration, and that extreme bony remodeling adjacent to the disc may promote facet cartilage recovery through offloading of the articular cartilage.

1 | INTRODUCTION

Although intervertebral disc degeneration (IVDD) has been comprehensively characterized, pathologic changes at the disc-vertebral interfaces and to the facet joints concomitant with IVDD have not been extensively studied. The disc itself is an often-cited source of back pain. However, a growing body of evidence suggests that degenerative changes to the adjacent vertebral endplates and posterior facet joints also contribute to the development of back pain.[1-3]

Each spinal motion segment contains two vertebral bodies, one intervening intervertebral disc, and two posteriorly-located facet joints. Between the vertebral bodies and the intervertebral disc exists an endplate interface composed of a layer of hyaline-like cartilage[4-6] and a layer of cortical bone in which the vasculature terminates.[6] Given that the avascular discs rely primarily on diffusion to transport nutrients and waste products in and out of this endplate, convective transport across the healthy endplate plays a critical role in maintaining the disc's normal metabolic environment.[7-9] It has been shown that spontaneous disruption of this endplate transport leads to disc degeneration.[10,11]

Located posterior to the disc and endplates, the facet joints play a role in both constraining the spine's total range of motion and transferring loads off the intervertebral discs during articulation.[12-14] The lumbar facet joints bear 20%–30% of the healthy motion segment's axial loads[15,16] and contribute up to 48% of the healthy motion segment's torsional stiffness during normal ambulation.[16] However, as the lumbar disc collapses during degeneration, up to 70% of the compressive force ends up being transmitted across the facet surface.[17] This abnormal mechanical stress may play a role in the development of facet osteoarthritis (OA), characterized most commonly by articular cartilage fibrillation, cartilage erosion, and chondrocyte hypertrophy as well as more severe changes to the whole joint, including osteophyte formation, subchondral fracture, and whole joint calcification.[2,18,19]

Human studies have demonstrated varying correlations between disc degeneration and facet OA. Some clinical studies propose that disc degeneration must precede facet degeneration. Fujiwara et al.[20] only observed facet OA adjacent to the most degenerative discs in a clinical evaluation of 14 patients, and a more extensive study of 93 patients with severe disc degeneration reported minor facet OA in only 48.2% of patients.[21] However, facet degeneration can occur adjacent to both healthy and degenerative discs—implying that disc and facet degeneration may occur simultaneously.[22-24] In 320 adults, it was reported that over 90% of individuals had some form of L4–L5 and L5–S1 facet degeneration, regardless of back pain status.[25] Critically, even though a study of 361 people found that most individuals who suffered from disc degeneration also suffered from facet OA, 10%–20% of individuals across all age groups suffered from OA of at least one facet without any concomitant disc degeneration.[26]

Since the progression of spinal degeneration is difficult to study in humans, animal models are often used to study changes to the endplates, discs, and facets during degeneration. Facet OA has been induced in rodent models by percutaneous puncture of the cartilage,[27] unilateral osteotomy of a single joint,[28] or injection of the joint with small molecules that modulate proteolysis or inflammation.[29-32] The majority of these rodent studies focused on characterizing pain in response to facet OA but did not investigate how facet OA impacted degeneration of the entire motion segment. Critically, aberrant mechanical loading of the motion segment can induce disc degeneration.[33-35] Other studies induced facet OA by mimicking the abnormal facet loads experienced during disc degeneration using either a high magnitude single cycle of compression at 160% body weight[36] or a low magnitude 8-weeks compression at 20% body weight.[37] These studies provide evidence that loading experienced by the whole motion segment affects the health of both disc and facet tissues. However, these rodent studies do not define the precise degenerative relationship between these two tissues.

Facet osteoarthritic changes have also been observed in response to acute annular incisions of sheep lumbar discs.[38] In a sheep model where lumbar discs were dorsally immobilized, progression of both facet degeneration and cartilage endplate thinning was observed after 6 and 26 weeks of abnormal loading.[39] Similarly, bony endplate thickening with disc degeneration has been measured in both human cadaveric[40,41] and clinical[42,43] studies. This suggests the bony endplates may become denser and the cartilage endplates thinner in response to reduced compressive stresses across the disc.[3] It remains unclear whether disc degeneration or endplate remodeling initiates the degenerative cascade.[42]

In both humans and animals, the occlusion of marrow channels and capillary buds in the endplate correlates with disc degeneration.[44-47] Ashinsky et al.'s[48] work in the rabbit disc puncture model illustrated a decrease in disc-adjacent vessel area as well as a thickening of the bony endplate, which ultimately led to a decrease in transport of small molecules across the endplate. Rabbits that underwent 28 days of fixed motion segment compression exhibited similar endplate thickening and vessel loss concurrent with

disc degeneration, suggesting the two pathologies may occur simultaneously in response to aberrant loading.[49]

Overall, cross-sectional studies of human tissues or subjects make it difficult to gain an understanding of how degeneration of a single element of the motion segment might affect the whole. Animal models are uniquely situated to study this crosstalk across a variety of time points. In these models a healthy disc can be perturbed in isolation of other factors that complicate clinical evaluations, such as age, gender, and lifestyle differences. Rabbit lumbar disc puncture is a well-established model for studying IVDD and its treatments.[50,51] The mechanical properties of rabbit discs more closely mimic those of human discs than other species do.[52] Rabbit lumbar motion segments also allow for the study of facet joint degeneration alongside disc degeneration, which is not possible in rodent tail models of IVDD due to a lack of posterior elements. Although not as clinically relevant as a goat or sheep model, the lower cost of the rabbit model makes it an attractive choice for the study of tissue crosstalk at multiple time points. Uniquely, the accelerated development of vertebral body osteophytes in this model[53–55] when compared to those that form more slowly or not at all in ovine models[38,56] may mimic a segment of the patient population that develops disc osteophytes in late-stage IVDD.[57–59] Thus far, most animal models of spinal degeneration have focused on understanding degenerative changes to one particular region within the spine (the disc, the endplate, or the facets) in isolation, limiting our understanding of the pathogenesis of disease.

The current study seeks to determine the crosstalk between these individual pathologies and IVDD by assessing two different severities of disc injury and subsequent degeneration over time. We hypothesized that degenerative changes to load bearing structures of the spine—the cartilage endplates and the facet joints—would follow altered mechanical loading created by acute disc injury and that the severity of these changes would be contingent on progressive degeneration of the disc.

2 | MATERIALS AND METHODS

2.1 | Surgical method and study design

The study design is summarized in Figure 1. Discs and facets spanning the same spinal levels as punctured in the in vivo studies were obtained from age-matched nonexperimental male New Zealand White rabbit spines (Sierra Medical, RSPI) as healthy controls. Control discs underwent tension-compression creep mechanical testing, μCT analysis, and paraffin histology, and control facet cartilage underwent creep indentation testing followed by paraffin histology. In addition to providing control discs, healthy rabbit spines also provided discs that underwent ex vivo puncture using either a 16G or 21G needle to evaluate acute mechanical changes in the disc immediately post-puncture. Mechanical changes were quantified through standard tension-compression and creep mechanical testing.[53,60]
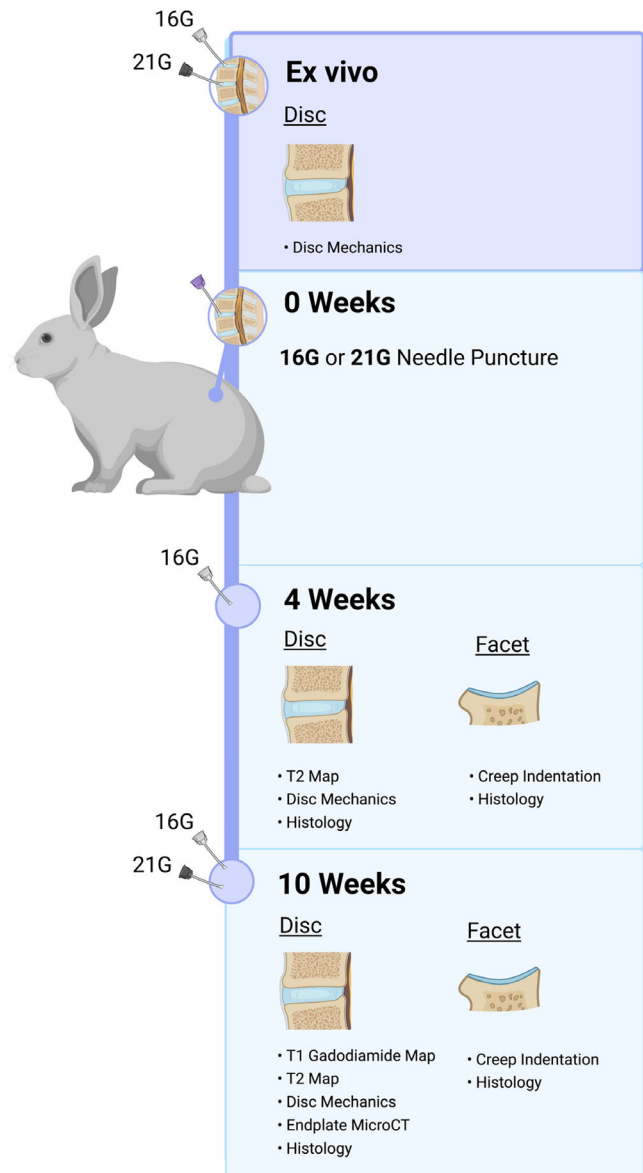

FIGURE 1 Study overview. Control discs were punctured ex vivo using either a 16G or 21G needle and then subject to mechanical testing. Disc and facet degeneration in response to acute annular injury with either a 16G or 21G needle in New Zealand White rabbits was assessed at 4 and 10 weeks post-puncture. 16G punctured discs and facets were assessed at both 4 and 10 weeks, while 21G punctured discs and facets were assessed at 10 weeks.

Surgery was performed on eight New Zealand White male skeletally mature rabbits (∼3 kg, ∼3 months of age) (Charles River Laboratories, Wilmington, MA) following guidelines established by the University of Pennsylvania's Institutional Animal Care Use Committee. The surgical method followed a previously established rabbit-puncture model.[53] In five rabbits, four levels between L23 and L67 with an average disc height of 2.17 mm, were punctured, two using a 16G needle and two using a 21G needle. The ratio of needle diameter to disc height was 0.377 (21G needle) and 0.760 (16G needle). Each needle was inserted 5 mm into the anterior AF and rotated 360°.

At 10 weeks post-puncture, prior to euthanasia, rabbits underwent coronal MRI post-contrast enhanced T_1 mapping and T_2 mapping to quantify small molecule diffusion across the endplate and disc T_2 relaxation times, respectively. Adjacent non-punctured discs between L23 and L67 were used as internal controls in the MRI dataset to reduce animal usage. Following euthanasia and dissection, 10-weeks post-puncture motion segments were then subjected to tension-compression creep mechanical testing, μCT analysis, and paraffin histology. Prior to MRI, facets were dissected away from the motion segments for creep indentation mechanical testing of the facet cartilage followed by paraffin histology.

Results from the initial 10 week study suggested that facet degeneration followed an unexpected progression of degeneration in the 16G group, unlike the degenerative trend observed in the endplates. Therefore, in three additional rabbits, two levels between L23 and L67 were punctured using a 16G needle to assess facet degeneration at an earlier time point. At 4 weeks post-puncture, these animals were euthanized, and the motion segments were dissected to separate the anterior column (vertebra—disc—vertebra) and posterior facet joints for characterization. Discs from these rabbits then underwent tension–compression creep mechanical testing followed by paraffin histology and the adjacent facet cartilage underwent creep indentation testing followed by paraffin histology.

2.2 | Disc and endplate characterization

2.2.1 | MRI

At 10 weeks post-puncture, animals were intravenously administered 0.3 mmols/kg of the small molecule, nonionic MRI contrast agent, gadodiamide (GE Healthcare, Omniscan™ (Gadodiamide) Injection, MW = 573), 30 min prior to euthanasia.[9,48] Immediately following euthanasia, vertebra—disc—vertebra segments were subjected to MRI scans at 4.7T to obtain mid-coronal images for T_1 relaxation mapping using an inversion recovery sequence (156 μm in-plane resolution, 1 mm slice thickness). T_1 relaxation time constants were quantified for a circular region of interest in the central nucleus pulposus. Gadodiamide is a T_1 shortening agent and, thus, a greater percent reduction in T_1 constant (discs without gadodiamide versus discs with gadodiamide) indicates an increase in gadodiamide diffusion into the disc. At the 10 weeks time point, mid-coronal slices for T_2 mapping (TE = $i \times 11.13$ ms, i = 1, 2, …16, where i indicates echo number; 156 μm in-plane resolution, 0.5 mm slice thickness) were also obtained, and average T_2 maps were generated using custom MATLAB software, as previously described.[61] The NP and AF regions were manually contoured along the NP–AF tissue boundary from the T_2 maps to calculate mean NP and AF T_2. T_2 relaxation times in the disc tissues are positively correlated with tissue water and proteoglycan content.[62] Following MRI, motion segments were then frozen at −20°C for subsequent characterization.

2.2.2 | Mechanical assessment

Vertebra—disc—vertebra segments were thawed and subjected to tension–compression creep mechanical testing consisting of 20 cycles of tension (21 N) and compression (42 N) at 0.5 Hz followed by a constant load of 42 N applied for 10 min using an Instron 5948 (Instron, Norwood, MA). Before testing, k wires (Smith & Nephew, 128010) were drilled into each disc's adjacent vertebral endplates to facilitate potting in a custom testing fixture using a low melting temperature indium casting alloy. Potted discs were then mounted in a water bath filled with 1X PBS (Invitrogen, 14190136). During testing, a high-resolution digital camera was used to capture deformation of the disc over time.

The 20th cycle of tension–compression as well as the entire creep test was analyzed using custom MATLAB software, which links the mechanical load applied by the Instron with the deformation captured by the camera, as previously described.[60,62] Analysis included total range of motion (TROM), compressive modulus (CMOD), neutral zone modulus (NZ MOD), and creep displacement. Measured load and motion-tracked displacement were converted to stress and strain by dividing each by the total cross-sectional area and height, respectively. Stress–strain curves were fit to a sigmoidal function, and boundaries of the neutral zone defined as the maximum and minimums of the second derivatives of this function. Compressive modulus and neutral zone modulus were defined as the slope of each of these regions defined by the sigmoidal fit. Total range of motion was defined as total displacement from the end of the compressive region to the end of the tensile region. Creep behavior was fit to a 5-parameter viscoelastic constitutive model, as previously defined.[60] Following mechanical testing, 10-weeks post-puncture motion segments were scanned using μCT, while 4-weeks post-puncture motion segments were prepped for paraffin histology. All vertebra—disc—vertebra segments were fixed in 10% buffered formalin (Sigma, HT501320) following mechanics.

2.2.3 | μCT

Samples were scanned using a Scanco Medical μCT 50 (Scanco Medical AG, Brüttisellen, Switzerland) to quantify bone morphometry at 10 μm isotropic resolution. Endplate volumes between the growth plate and the disc were manually contoured by blinded individuals to quantify bone volume fraction and trabecular morphometry parameters, including trabecular number, thickness, and spacing, as previously described.[48] Osteophytes were separately contoured to quantify total bone volume.

2.2.4 | Histology

Following μCT, discs were decalcified in Formical (StatLab Medical Products, 1314) and processed for paraffin histology using a Leica ASP300S Tissue Processor (Leica Microsystems, Buffalo Grove, IL).

Samples were sectioned at a thickness of 10 μm in the sagittal plane and stained with Hematoxylin/Eosin and Safranin-O/Fast Green. Disc histology was scored by a blinded panel using a 3-scorer consensus system according to the ORS Spine Section intervertebral disc scoring system.[51] Scores were aggregated into three categories to form individual NP, AF, and EP scores and summed to create an overall score (Figure 3B; see Figure S2 for stratification of scores). The JOR Spine/ ORS Spine Section intervertebral disc scoring system for the rabbit model[51] is comprised of seven different assessments. Scores for NP shape, NP area, NP matrix condensation, and NP cell number contributed to the overall NP score. Scores for AF/NP border and AF morphology contributed to the overall AF score, and a score for EP sclerosis/thickening contributed to the overall EP score.

2.3 | Facet characterization

2.3.1 | Mechanics

Creep indentation mechanical testing[63,64] was performed at one point on each facet articular surface to quantify changes in cartilage mechanical properties. Facets were potted using a low melting temperature indium casting alloy and indented while immersed in 1X PBS. A compressive creep load of 0.1 N was applied for 15 min through a 2 mm diameter spherical indentation testing rig coupled with an Instron 5948 (Instron, Norwood, MA).

Mechanical properties of the facet cartilage were calculated by fitting the displacement versus time curves to a Hertzian biphasic creep model.[65] From that model, the hydraulic permeability (k_0), the nonlinear strain-dependent flow-limited constant (M), the tensile modulus (E_{Y+}), and the compressive modulus (E_{Y-}) were calculated. A least squares regression was performed on the creep data to determine the best-fit k_0 and M values for each facet; indentation tests that resulted in an R^2 value of less than 0.97 were excluded from the analysis (excluded 7 of 58 indentation tests).

2.3.2 | Histology

Facets were then fixed in 10% buffered formalin, decalcified, and processed for paraffin histology as outlined in Section 2.2.4. Facets were then sectioned in the sagittal plane at a thickness of 10 μm and stained with Safranin-O/Fast Green. Histology images were scored using a 3-scorer consensus system according to the OARSI scoring system for rabbit cartilage.[66]

2.4 | Data analysis

All data was analyzed using a D'Agostino–Pearson omnibus normality test followed by a one-way ANOVA with a Tukey's or Dunn's post hoc test for normally or non-normally distributed datasets, respectively, in GraphPad Prism 9. Graphs show mean plus standard deviation.

3 | RESULTS

Each intervertebral disc underwent tension–compression and creep mechanical testing. Figure 2A illustrates an increased range of motion (+97%) immediately following a 16G acute injury, compared to uninjured controls. Notably, acute injury with a smaller 21G needle only marginally increased disc total range of motion (+72%), but this increase was not significant in comparison to uninjured controls. As time progressed in vivo, 16G discs showed a significant reduction in mobility (Figure 2A; −53% at 4 weeks, −64% at 10 weeks compared to 16G acute puncture) corresponding with a significant increase in neutral zone modulus (Figure 2B; +507% at 4 weeks, +746% at 10 weeks compared to 16G acute puncture). Although 21G discs showed a similar trend, these changes were not statistically different from uninjured controls or the 21G acutely punctured discs. No statistically significant differences in compressive moduli were found between any experimental groups (Figure 2C). Creep displacement was reduced in both 16G (−64%) and 21G (−59%) punctured discs when compared to controls at 10 weeks (Figure 2D). When discs were analyzed using MRI T_2 mapping, both puncture groups showed a progressive loss of T_2 signal in the NP, with a more severe reduction occurring in 16G discs (−52%) than in 21G discs (−42%) at 10 weeks (Figure 2E,F). Interestingly, NP T_2 relaxation times, which correlate with NP proteoglycan and water content,[54] were comparable between the 16G punctured group at 4 weeks and the 21G punctured group at 10 weeks.

All disc histology was scored by blinded reviewers. Scores were aggregated into three categories to form individual NP, AF, and EP scores and summed to create an overall score (Figure 3B; see Figure S2 for stratification of scores). The JOR Spine/ORS Spine Section intervertebral disc scoring system for the rabbit model[51] is comprised of 7 different assessments. Scores for NP shape, NP area, NP matrix condensation, and NP cell number contributed to the overall NP score. Scores for AF/NP border and AF morphology contributed to the overall AF score, and a score for EP sclerosis/thickening contributed to the overall EP score. All experimental discs were significantly more degenerative than control discs. Histology scores of 4-weeks 16G, 10-weeks 16G, and 10-weeks 21G punctured discs were 9X, 7.5X, and 4.13X higher, respectively, than histology scores of control discs. The highest, and most degenerative, histology scores occurred in the 4-weeks 16G puncture group, and these were driven by changes across all three disc compartments. This can be seen in representative histology images (Figure 3A; see Figures S1 and S2 for additional histology images). Safranin-O/Fast Green histology of all 4-weeks 16G punctured discs (Figure S1) showed no definitive NP tissue, which can be distinctly seen in control samples. Further examination with Hematoxylin and Eosin revealed serpentine and sometimes ruptured AF lamellae with little to no distinction between NP and AF regions of the disc, as well as a thickening of the cartilage endplate cell layer. 16G punctured discs were similarly degenerative at 10 weeks as at 4 weeks but had less degenerative cartilage endplates at 10 weeks.
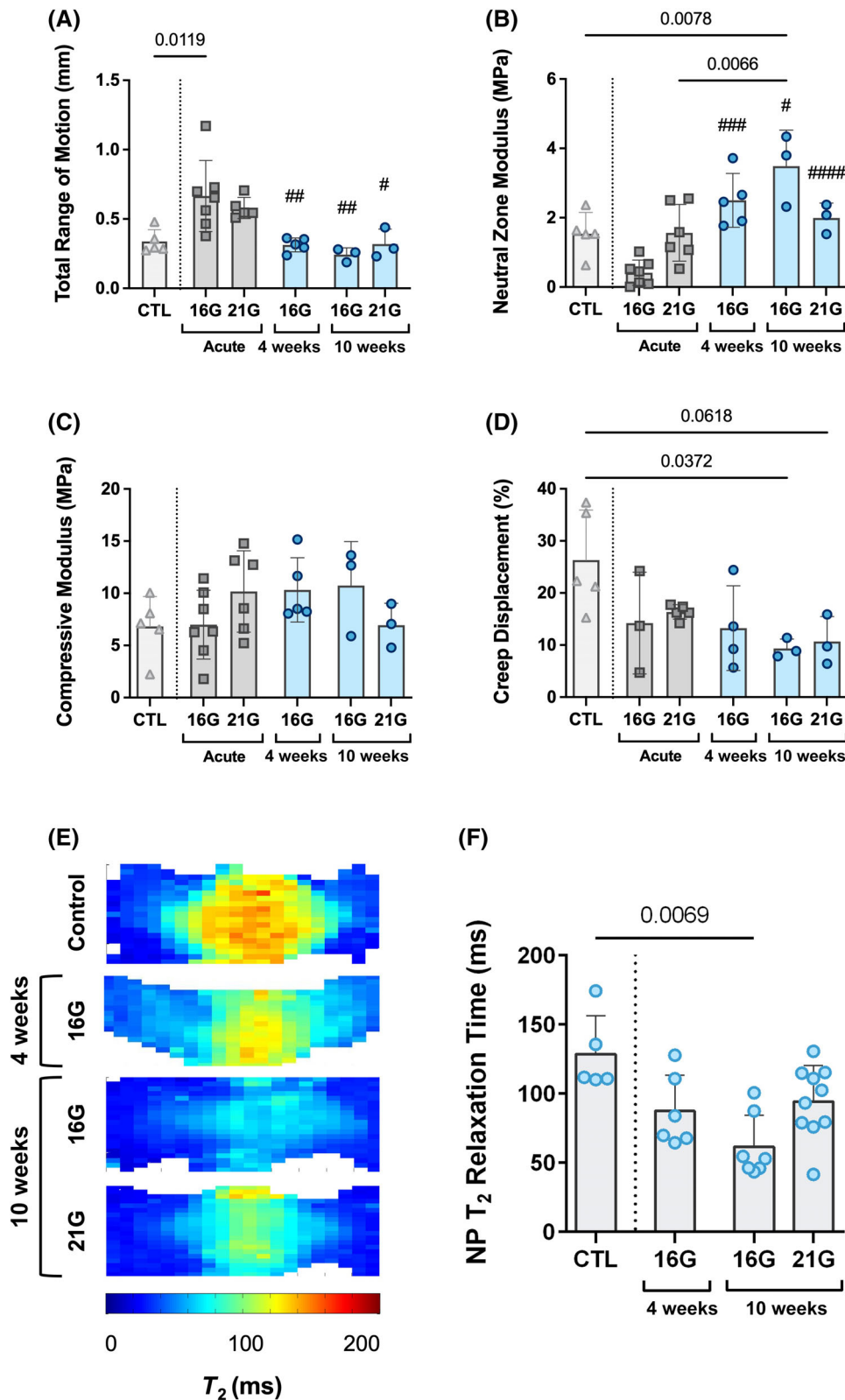
FIGURE 2 Disc mechanics.
(A) Total range of motion,
(B) neutral zone modulus,
(C) compressive modulus, and
(D) creep displacement of discs.
(E) Composite T_2 maps of disc NP
and AF regions ($n = 5$–10), and
(F) NP T_2 relaxation time. (#
indicates $p < 0.05$ vs. 16G acute
discs; ## indicates $p < 0.01$ vs. 16G
acute discs; ### indicates $p < 0.001$
vs. 16G acute discs; and ####
indicates $p < 0.0001$ vs. 16G acute
discs).

Histology scores were significantly lower in 21G punctured discs at 10 weeks compared to 16G punctured discs at both 4 weeks (52% lower) and 10 weeks (42% lower). This reduction was driven by all three compartments of the disc (Figure 3B). The NP in the 21G punctured discs retained its shape, area, and cell density as well as a more gelatinous matrix compared to the 16G punctured NPs at either time point. Most of the 21G punctured discs experienced small regions of serpentine AF lamellar disorganization combined with small loss of distinction between the AF and NP. Cartilage endplates were similarly degenerative in both 16G and 21G punctured groups at
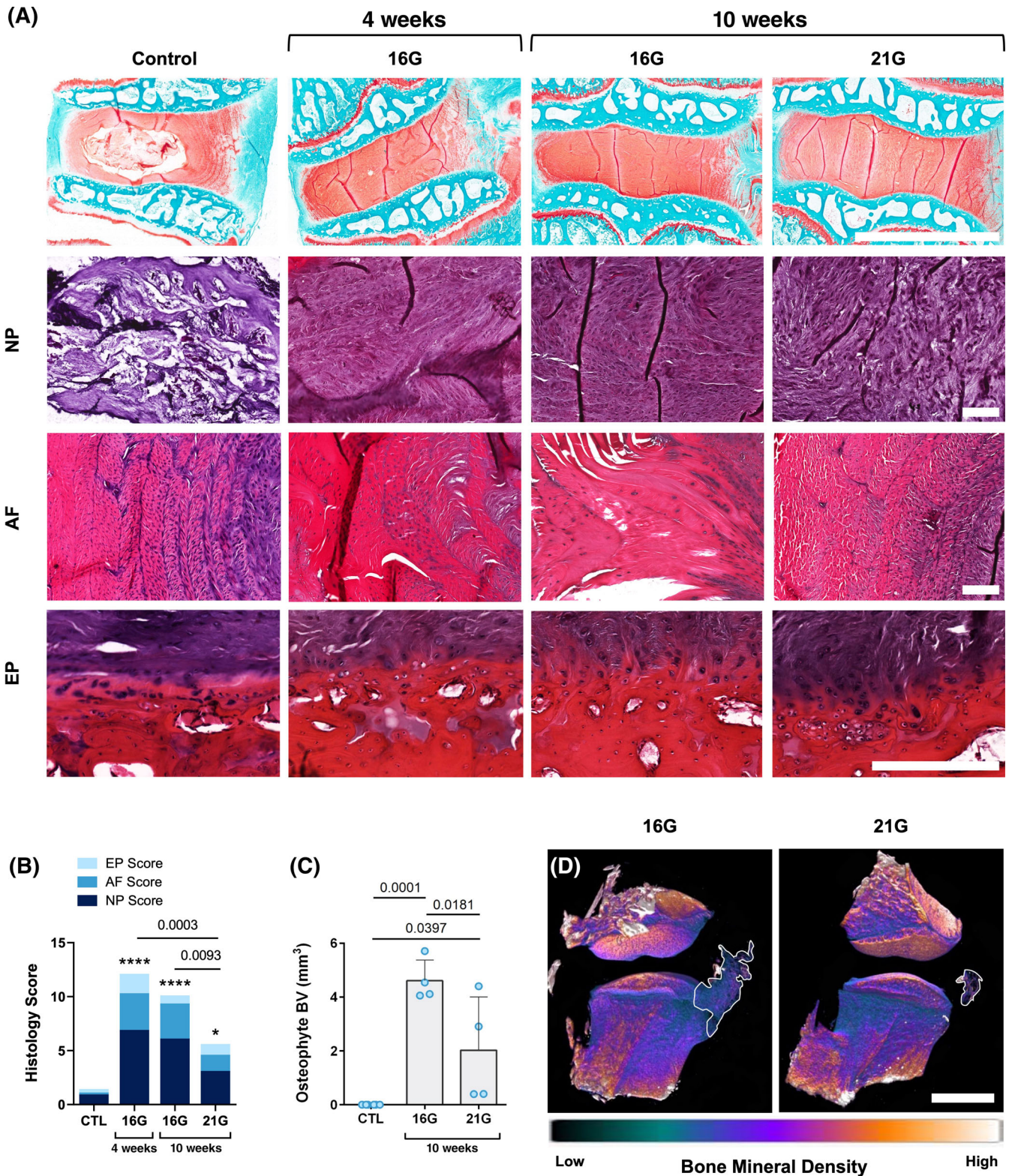
FIGURE 3 Disc tissue changes. (A) Safranin-O/Fast Green histology of the entire disc (scale = 4 mm) for all experimental groups, as well as representative Hematoxylin and Eosin histology of disc NP, AF, and EP regions (scale = 200 μm). (B) Total ORS Spine section intervertebral disc score stratified by NP, AF, and EP regions (n = 4–6). (C) Osteophyte μCT bone volume quantification and (D) representative μCT reconstructions of 10-weeks 16G and 21G punctured discs, with osteophyte volumes contoured in white (scale = 3 mm). (* indicates $p < 0.05$ vs. control discs; **** indicates $p < 0000.1$ vs. control discs).
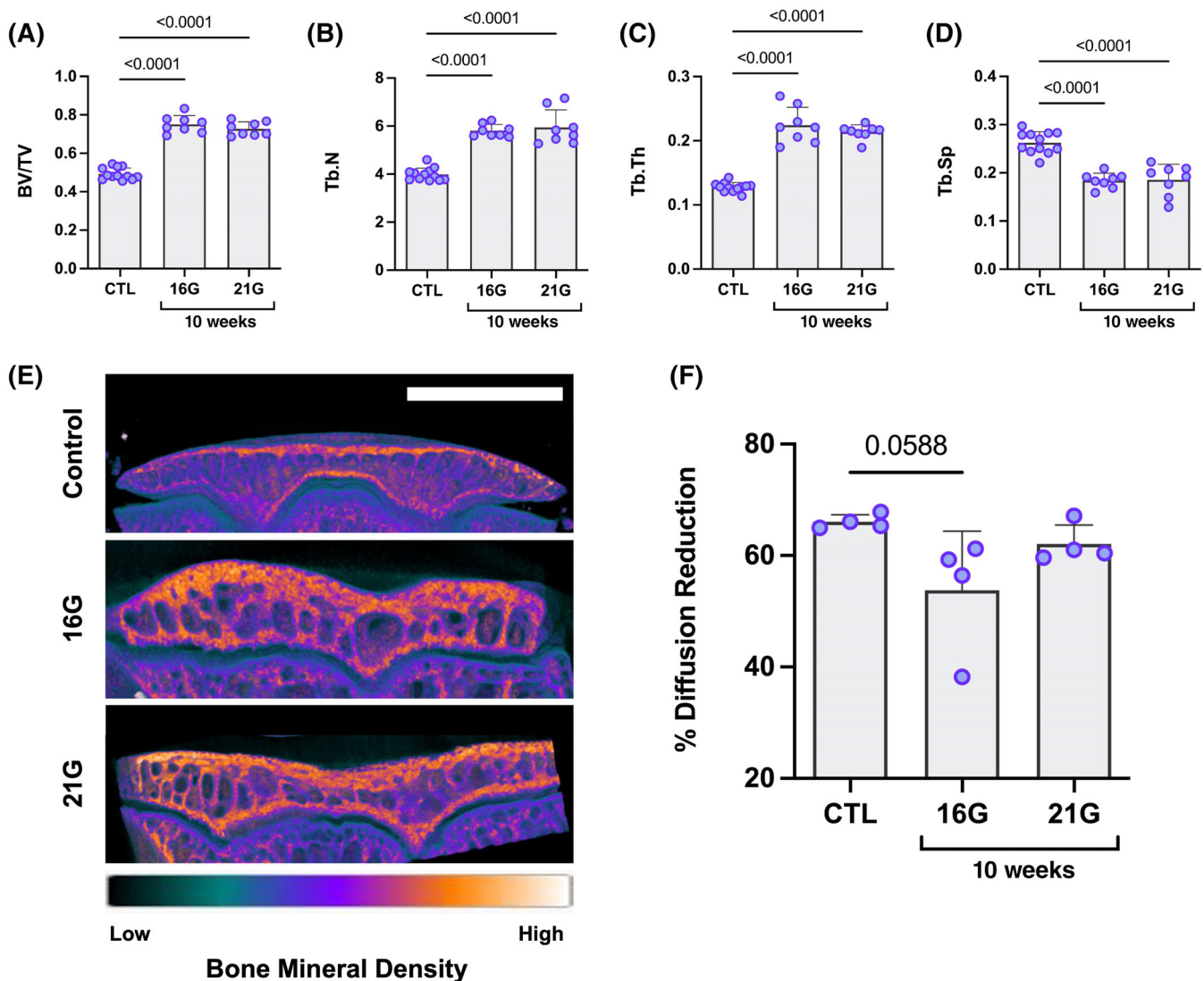
FIGURE 4 Bony endplate changes. μCT quantification of (A) bone volume fraction, (B) trabecular number, (C) trabecular thickness, and (D) trabecular spacing, as well as (E) representative μCT cross-sections (scale = 2 mm) of bony endplates adjacent to control and 10-weeks 16G and 21G punctured discs. (F) Percent reduction in T_1 relaxation time of the NP following gadodiamide administration.

10 weeks. The 21G punctured discs were more degenerative than control discs, due most prominently to increased NP matrix condensation in all punctured samples (Figure S2).

Osteophyte formation was observed anteriorly on all 10-weeks punctured discs. Discs punctured with a 16G needle formed bony osteophytes with a significantly larger volume than discs punctured with a 21G needle (Figure 3C), as can be seen in representative μCT reconstructions (Figure 3D). The presence of immature, cartilaginous osteophytes bridging across the outer AF were also observed in 16G punctured discs at both time points (Figure S3).

The bony endplates adjacent to injured discs of both experimental groups experienced significant sclerotic changes by 10 weeks. Bone volume fraction was increased by 50% in endplates adjacent to 21G punctured discs and by 52% in endplates adjacent to 16G punctured discs in comparison to uninjured controls (Figure 4A). This increase in bone volume was driven by a concomitant increase in trabecular

number (Figure 4B), increase in trabecular thickness (Figure 4C), and decrease in trabecular spacing (Figure 4D) as can be seen in representative μCT cross-sections (Figure 4E). No differences in bone volume fraction were observed between 16G and 21G punctured groups. A corresponding progressive reduction in small molecule diffusion into the disc with increasing puncture diameter accompanied the increase in bone volume fraction (Figure 4F). Gadodiamide diffusion was decreased more in 10-weeks 16G punctured discs (−19%) than in 10-weeks 21G punctured discs (−6%) when compared to control discs. Although gadodiamide diffusion was not significantly reduced in the 21G punctured discs, a small reduction in transport was observed.

Overall, facets adjacent to 4-weeks 16G punctured discs and facets adjacent to 10-weeks 21G punctured discs were similarly degenerative, and were more degenerative than facets adjacent to 10-weeks 16G punctured discs for every metric analyzed. No changes were found in facet cartilage tensile modulus across any group or time
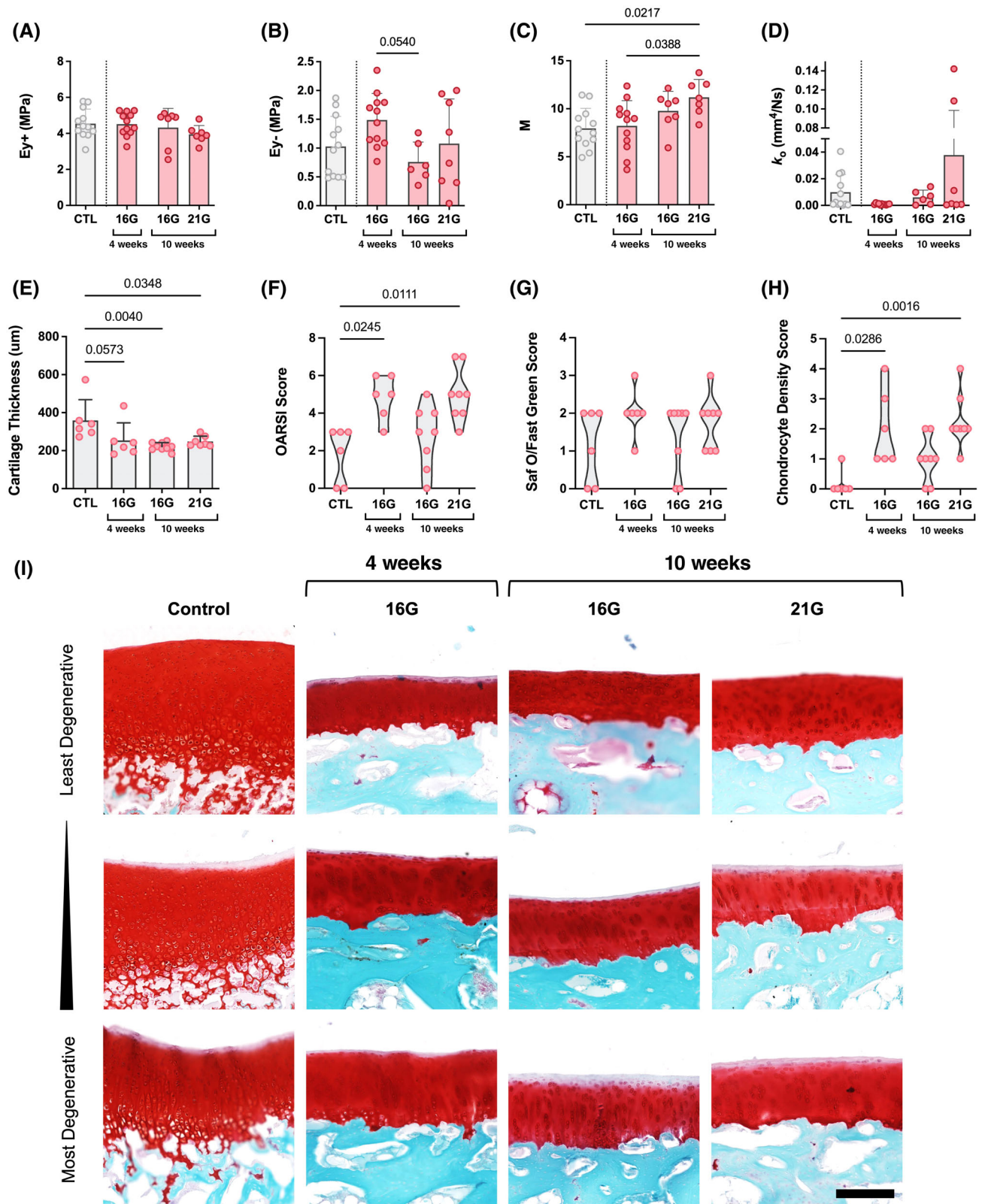
FIGURE 5 Facet cartilage changes. (A) Tensile modulus, (B) compressive modulus, (C) strain-dependent flow-limited constant, and (D) hydraulic permeability of the facet articular cartilage measured by indentation testing. (E) Cartilage thickness. (F) OARSI score of facet Safranin-O/Fast Green histology as well as histology scores stratified by individual (G) Safranin-O/Fast Green score and (H) chondrocyte density score. (I) Least, mid, and most degenerative Safranin-O/Fast Green histology of facet articular cartilage for all experimental groups (scale = 200 μm).

TABLE 1 Selected results from the Pearson correlation matrix between quantitative disc, endplate, and facet outcome metrics.

Parameter 1	Parameter 2	Pearson correlation coefficient (r)	p value (p)
Disc compressive modulus	Facet cartilage tensile modulus	0.6	0.014
Disc NP T_2 relaxation time	Facet cartilage tensile modulus	-0.722	0.043
Disc compressive modulus	Endplate diffusion into NP	-0.842	0.035
Disc creep displacement	Endplate bone volume/total volume	-0.815	0.002
Disc neutral zone modulus	Endplate bone volume/total volume	0.637	0.035
Disc NP T_2 relaxation time	Disc total range of motion	0.747	0.026

point (Figure 5A). However, a reduction in average cartilage compressive modulus (-37%) was observed in facets adjacent to 16G punctured discs from 4 to 10 weeks (Figure 5B). An increase in both the strain-dependent permeability factor (M) and permeability (k_0) was observed in the 10-weeks 21G facets when compared to controls (Figure 5C,D), and this increased permeability was significant only for M. M increased by 27% and 23% in 10-weeks 21G facet cartilage when compared to controls and 4-weeks 16G facet cartilage, respectively. A trending increase in both M and k_0 was also observed in the facets adjacent to 16G punctured discs with increasing time. Cartilage thinned greatly by 4 weeks (29% thinner) and significantly by 10 weeks in facets adjacent to both 16G (39% thinner) and 21G (34% thinner) punctured discs when compared to controls (Figure 5E).

Facet histology was graded using the OARSI scoring system,[66] which quantifies Safranin-O/Fast Green staining, tissue structure, and chondrocyte density. Overall, 4-weeks 16G facets (155% higher OARSI score than controls) and 10-weeks 21G facets (118% higher OARSI score than controls) were similarly degenerative and significantly more degenerative than facets adjacent to uninjured controls (Figure 5F). In comparison, 10-weeks 16G facets were only 18% more degenerative than controls according to OARSI score. No measurable changes in Safranin-O/Fast Green staining occurred over time, although the data followed the same trend as in the composite OARSI score (Figure 5G). Ultimately, chondrocyte density was the main driver of overall facet OARSI score (Figure 5H; see Figure S4A). Compared to controls, a loss of chondrocytes was noted in all groups with an increase in irregular cell organization only occurring in 4-weeks 16G and 10-weeks 21G facets, as can be seen in the Safranin-O/Fast Green images (Figure 5I). The tissue structure score trended higher in 21G facets at 10 weeks, but no groups were significantly different (see Figure S4B).

A Pearson correlation matrix was generated to elucidate correlations between the disc, endplate, and facet outcomes across all experimental groups (Table 1; see Figure S5 for complete correlation matrix). Facet articular cartilage tensile modulus positively correlated with disc compressive modulus ($r = 0.6$, $p = 0.014$) and negatively correlated with disc NP T_2 relaxation time ($r = -0.722$, $p = 0.043$). Compressive modulus of the disc increased as diffusion into the NP decreased ($r = -0.842$, $p = 0.035$). Endplate bone volume fraction correlated with two disc parameters: creep displacement and neutral zone modulus. Bone volume fraction was negatively correlated with

disc creep displacement ($r = -0.815$. $p = 0.002$) and positively correlated with changes to disc neutral zone modulus. NP T_2 relaxation time positively correlated with disc total range of motion.

4 | DISCUSSION

Degeneration in the disc's adjacent vertebral endplates and posterior facet joints has been hypothesized as a contributing factor in the development of back pain.[1–3] However, exactly how these compartments of the motion segment engage in crosstalk with the disc following disc injury remains unclear. Results from this study reinforce the well-documented phenomenon that acute disc injury compromises disc mechanical function, leading to disc degeneration, the severity of which increases with both needle diameter and time.[53,67] The adjacent vertebral endplates underwent increasingly severe remodeling in response to increasingly traumatic disc injury. However, facet cartilage did not follow this same trend. Our results suggest that degenerative changes within all three compartments of the motion segment are dependent on both the presence of osteophytes and the disruption of healthy disc matrix. Degenerative differences observed in facets from different injury groups may be attributed in part to altered magnitudes of loading experienced by the spine's posterior elements following disc remodeling.

The rabbit puncture model results in stiffening of injured discs as a result of matrix remodeling in the AF[53] and NP as well as formation of anterior osteophytes.[53] As seen in other studies using this model, changes in disc function and structure were time dependent.[53,68] The progression of disc degeneration also depended on the degree of injury. Overall, discs punctured with a larger 16G needle experienced more severe degeneration than discs punctured with a smaller 21G needle. A similar percutaneous rabbit injury model demonstrated that the needle puncture caused lamellar disorganization of the AF, which led to loss of a distinct border between the AF and NP,[69] as observed in this study. 16G punctured discs also experienced higher levels of osteophyte formation compared to the 21G punctured discs at 10 weeks.

Consistent with our prior work in this model at a 12 week time point, disc puncture led not only to alterations in NP and AF tissue structure but also to sclerosis of the bony endplates and reduced small molecule transport into the disc.[48] Endplate bone volume

fraction increased in both experimental groups compared to the uninjured controls at 10 weeks. Due to this increase in bone density, small molecule diffusion into the disc decreased. Although small molecule diffusion across the endplate into the 21G punctured discs was not significantly reduced in comparison to controls, a small reduction in transport was still observed. The significant reduction in transport observed in the 16G punctured discs may be attributed to remodeling of the cartilage endplate in addition to bony endplate sclerosis. Although not measured during the course of this study, remodeling of the cartilage endplate is known to limit diffusion into the disc via compositional defects, such as increased collagen and Aggrecan content[70] or tissue calcification.[6] Similarly, artificially increasing endplate density of both the cartilaginous and bony endplate via cement injection into large animals interfered with endplate vasculature and blocked nutrient transport.[45,47]

Humans often experience endplate sclerosis due to a loss of osteochondral integrity, caused by increased bone deposition and cartilage calcification.[71,72] Previous cadaveric work determined that subchondral bone becomes denser in association with disc degeneration,[40] an observation similar to those made throughout the course of this study. However, the time course of these bony changes in humans is unclear. It is likely that progressive endplate remodeling occurs concomitantly with progressive disc degeneration, as stiffening of the disc is correlated both with increased bone volume fraction and with reduced transport across the endplate.

Although the bony endplates followed a path of progressive degeneration in response to increasingly severe disc injury, the facet cartilage did not follow this same trend. Persistent significant thinning of the facet cartilage in all experimental groups was the only strong indicator of cartilage degeneration, indicating that every experimental facet experienced lasting degeneration during the course of the study. The progression of facet articular cartilage degeneration has not been well documented.[73] Knee OA, however, has been extensively studied and can provide insight into the facet changes observed over the course of this study. Progressive softening of articular cartilage of the human femoral condyle occurs as OA develops,[74–76] and this softening often corresponds with a loss of glycosaminoglycans.[77] Similar articular cartilage softening was measured in human facets with severely degenerative Grade 4 and 5 OARSI scores.[64] Over the course of this study a significant loss of compressive or tensile stiffness was not observed in facets of any group. More severe cartilage OA than was observed here is likely required to measure changes in cartilage modulus, as joints that do experience a reduction in compressive modulus have already undergone severe osteoarthritic changes. Despite this, facet cartilage tensile modulus was positively correlated with increased disc compressive modulus and negatively correlated with NP T_2 relaxation time, supporting the hypothesis that disc and facet remodeling are intertwined.

Only facet tensile modulus was significantly correlated with disc properties when analyzed using a Pearson correlation matrix. However, changes to other facet properties, including the cartilage nonlinear strain dependent flow limited constant (M) and OARSI score, correlated significantly with changes to endplate bone volume fraction. Over the course of this study facet and endplate degeneration was observed asynchronous with progressive disc degeneration. This delay in degeneration coupled with the fact that facet OA was minimal overall most likely explains the lack of correlation between many disc and facet cartilage properties.

The most severely degenerative rabbit facets in this study were only mildly degenerative, experiencing minor fibrillation and areas of focal chondrocyte reorganization. Ultimately, the most degenerative cartilage was observed over the course of this study in facets adjacent to 21G punctured discs at 10 weeks, where we observed increased permeability of the facet cartilage compared to both control and 4-weeks 16G facets. Increases in cartilage permeability have been observed at early stages of OA in cadaver knees.[78] This increase in permeability has also been documented previously in degenerative human facets[64] and knees[79] as well as in both affected and contralateral joints of a rabbit anterior cruciate ligament transection OA model.[80] Although cartilage histology and indentation mechanics begin to capture the mild degeneration seen in response to this disc injury model, OA is more than a disease of the cartilage. Other markers of disease progression in the synovium[81,82] or ligamentous joint capsule may be more sensitive to capturing this early-stage OA[83] and may better elucidate the progression of disease from degeneration to recovery.

As the facet joints were initially unperturbed in this disc injury model, our results suggest that disc-facet biomechanical crosstalk contributes to the initiation of early-stage facet OA. It has been shown that loss of disc height increases mechanical stress across the articular surfaces of the facet joint by creating areas of focally magnified compressive load[20,84,85] and that disc degeneration causes facet hypermobility which may contribute to increased stresses during facet articulation.[86] Continuous loading of the facet articular cartilage (up to 10 000 cycles) can result in surface fibrillation.[87] The increased disc mobility that we observed immediately following puncture in the 16G group also likely contributed to the development of facet OA seen at 4 weeks.[88] The formation of mature boney osteophytes and immature, cartilaginous osteophytes that bridged anteriorly as time progressed in vivo likely reduced this overloading of the facet cartilage by distracting the joint and contributing to increased disc stiffness overall. The development of anterior osteophytes past 4 weeks is consistent with previous observations of this model.[53–55] Both osteophyte size and disc stiffness were greater in 16G punctured discs than in 21G punctured discs at 10 weeks. 21G punctured discs were less degenerative than 16G punctured discs, creating a mechanical environment where aberrant loading across the motion segment likely contributed to increased loading on the facet joints over a longer period, culminating in early-stage facet OA.

The formation of mature and immature osteophytes in the anterior AF is thought to reduce loading across the facet joint through their contribution to disc stiffness. The partial recovery of facet cartilage health from 4 to 10 weeks in the 16G puncture group is believed to be a direct result of this phenomenon; prior studies of offloading in the knee joint document similar observations of cartilage recovery following reduced joint loading.[89–92] Offloading treatments aim to

reduce abnormally high stress levels across misaligned or overly compressed joint surfaces while maintaining a healthy level of hydrostatic loading to stimulate cellular anabolism. Conservative clinical approaches aimed at treating suspected facet pain involve unloading the facet cartilage during physical therapy.[93] Offloading in the knee can be accomplished permanently through high tibial osteotomy[89,90] or temporarily through joint distraction.[91] Patellofemoral realignment in the knee through osteotomy increased cartilage glycosaminoglycan content over a 2-year period.[89] Cartilage recovery has also been observed in rats,[94] rabbits,[95] and dogs[96] following joint distraction. Notably, as was observed in this study, Moore et al.[38] also showed that the development of facet cartilage OA in sheep was driven by disruptions to normal chondrocyte organization and that without the formation of osteophytes, the facet cartilage progressively degenerated. Although the facet cartilage adjacent to 16G punctured discs showed signs of recovery between 4 and 10 weeks, it did not experience a concomitant increase in cartilage thickness. It remains unclear whether this cartilage would fully recover if given enough time or if the significant reduction in cartilage thickness would prove irreversible.

Albeit useful for studying compartments of the motion segment in isolation, this rabbit model has limitations. Most prominently, the human motion segment can deteriorate for a variety of reasons, many of which may involve facet or endplate degeneration simultaneous with or even prior to disc degeneration.[20,21,24–26] Although a study of 535 human patients established a clinical association in humans between the presence of lumbar disc osteophytes and endplate sclerosis,[97] the formation of osteophytes and their associated bridging collagenous matrix in these rabbits far outpaces what would typically be seen in humans.[57–59,98]

Additionally, in this model, facet OA can only be studied in response to mechanical disc injury. Alternative models of IVDD induction include whole motion segment immobilization,[39] whole motion segment overloading,[37,49,50,99,100] intradiscal injection of chondroitinase ABC,[56,101,102] and intradiscal injection of proinflammatory molecules.[103] Overloading has been used in many rodent models[37,50,99] as well as rabbit models,[49,100] allowing for the study of simultaneous disc and facet perturbation. However, intradiscal injection of chondroitinase ABC, an enzyme that cleaves chondroitin sulfate proteoglycans, is a more popular method of inducing IVDD in large animals due to its ability to initiate the loss of proteoglycans as is seen in the onset of human IVDD.[56,102] In rabbits, formation of disc osteophytes in this chondroitinase ABC model is also much less severe than in the disc puncture model.[101] However, a comparative study of four different rabbit injury models, showed that annular puncture produced the most consistent degeneration.[104]

The results from this work emphasize that researchers looking to use the rabbit disc puncture model to study the treatment of disc or facet degeneration consider whether the developing pathology is physiologically relevant to the study questions they seek to address. It is clear that other structures of the spine outside of the disc should be considered in studies assessing tissue regeneration, as these structures also undergo degenerative changes in conjunction with disc degeneration.

Researchers looking to study the treatment of facet OA would need to use a less severe disc puncture with a 21G needle to incite progressive facet degeneration. Notably, this injury model in rabbits may not be suitable for testing the injection of living cells into the nucleus pulposus,[105] as is commonly investigated,[106] in the pursuit of cell-mediated tissue repair, given the reduction in small molecule transport that occurs in discs punctured with a 16G needle. Investigators will need to decide what tissue environments (early-stage degenerative vs. late-stage degenerative) are best suited for their study. Puncture with a 16G needle will create a model of IVDD with limited nutrient transport into the disc and, ultimately, a more hostile environment for cells to survive. Puncture with a 21G needle will create a model of IVDD with healthier nutrient transport into the disc and a less hostile environment in which to test cells. Considering that the rabbit disc continues to degenerate in an accelerated manner in response to puncture, a different model entirely may be more appropriate for replicating the pathology of early onset human IVDD in which many cell therapies would be clinically applied.

Overall, this study reinforces the fact that degeneration spans the whole spinal motion segment following disc injury, and is not limited only to the disc itself. Vertebral endplate thickening also occurs in response to disc injury, which ultimately limits the diffusion of small molecules into the disc. Our work also suggests that altered disc mechanics can induce facet degeneration, and that extreme bony remodeling of the disc may offload the facet joint and promote cartilage recovery.

CONFLICT OF INTEREST STATEMENT

Robert L. Mauck is Co-editor in Chief of JOR Spine. Sarah Gullbrand is an Editorial Board member of JOR Spine and co-author of this article. They were excluded from editorial decision-making related to the acceptance of this article for publication in the journal.

ORCID

Harvey E. Smith https://orcid.org/0000-0003-0488-2541
Sarah E. Gullbrand https://orcid.org/0000-0001-7806-6606

REFERENCES

1. Suri P, Hunter DJ, Rainville J, Guermazi A, Katz JN. Presence and extent of severe facet joint osteoarthritis are associated with back pain in older adults. *Osteoarthr Cartil.* 2013;21(9):1199-1206. doi:10.1016/j.joca.2013.05.013

2. Gellhorn AC, Katz JN, Suri P. Osteoarthritis of the spine: the facet joints. *Nat Rev Rheumatol*. 2013;9(4):216-224. doi:10.1038/nrrheum.2012.199

3. Zehra U, Robson-Brown K, Adams MA, Dolan P. Porosity and thickness of the vertebral endplate depend on local mechanical loading. *Spine*. 2015;40(15):1173-1180. doi:10.1097/BRS.0000000000000925

4. Roberts S, Menage J, Urban JPG. Biochemical and structural properties of the cartilage end-plate and its relation to the intervertebral disc. *Spine*. 1989;14(2):166-174. doi:10.1097/00007632-198902000-00005

5. Moon SM, Yoder JH, Wright AC, Smith LJ, Vresilovic EJ, Elliott DM. Evaluation of intervertebral disc cartilaginous endplate structure using magnetic resonance imaging. *Eur Spine J*. 2013;22(8):1820-1828. doi:10.1007/s00586-013-2798-1

6. Fields AJ, Ballatori A, Liebenberg EC, Lotz JC. Contribution of the endplates to disc degeneration. *Curr Mol Biol Rep*. 2018;4(4):151-160. doi:10.1007/s40610-018-0105-y

7. Maroudas A, Stockwell RA, Nachemson A, Urban J. Factors involved in the nutrition of the human lumbar intervertebral disc: cellularity and diffusion of glucose in vitro. *J Anat*. 1975;120(Pt 1):113-130.

8. Ferguson SJ, Ito K, Nolte LP. Fluid flow and convective transport of solutes within the intervertebral disc. *J Biomech*. 2004;37(2):213-221. doi:10.1016/S0021-9290(03)00250-1

9. Gullbrand SE, Peterson J, Mastropolo R, et al. Low rate loading-induced convection enhances net transport into the intervertebral disc in vivo. *Spine J*. 2015;15(5):1028-1033. doi:10.1016/j.spinee.2014.12.003

10. Gruber HE, Ashraf N, Kilburn J, et al. Vertebral endplate architecture and vascularization: application of micro-computerized tomography, a vascular tracer, and immunocytochemistry in analyses of disc degeneration in the aging sand rat. *Spine*. 2005;30(23):2593-2600. doi:10.1097/01.brs.0000187877.30149.83

11. Gruber HE, Phillips R, Ingram JA, Norton JH, Hanley EN. Spontaneous age-related cervical disc degeneration in the sand rat. *Clin Orthop*. 2014;472(6):1936-1942. doi:10.1007/s11999-014-3497-x

12. Gregersen GG, Lucas DB. An in vivo of the axial rotation of the human thoracolumbar spine. *J Bone Joint Surg Br*. 1967;49-A(2):247-262.

13. Fujiwara A, Lim TH, An HS, et al. The effect of disc degeneration and facet joint osteoarthritis on the segmental flexibility of the lumbar spine. *Spine*. 2000;25(23):3036-3044. doi:10.1097/00007632-200012010-00011

14. Ashinsky B, Smith H, Mauck R, Gullbrand S. Intervertebral disc degeneration and regeneration: a motion segment perspective. *Eur Cell Mater*. 2021;41:370-387. doi:10.22203/eCM.v041a24

15. Pal GP, Routal RV. Transmission of weight through the lower thoracic and lumbar regions of the vertebral column in man. *J Anat*. 1987;152:93-105.

16. Asano S, Kaneda K, Umehara S, Tadano S. The mechanical properties of the human L4–5 functional spinal unit during cyclic loading: the structural effects of the posterior elements. *Spine*. 1992;17(11):1343-1352. doi:10.1097/00007632-199211000-00014

17. Adams MA, Hutton WC. The mechanical function of the lumbar apophyseal joints. *Spine*. 1983;8(3):327-330. doi:10.1097/00007632-198304000-00017

18. Kirkaldy-Willis WH, Farfan HF. Instability of the lumbar spine. *Clin Orthop*. 1982;165:110-123.

19. Kalichman L, Li L, Kim DH, et al. Facet joint osteoarthritis and low back pain in the community-based population. *Spine*. 2008;33(23):2560-2565. doi:10.1097/BRS.0b013e318184ef95

20. Fujiwara A, Tamai K, Yamato M, et al. The relationship between facet joint osteoarthritis and disc degeneration of the lumbar spine: an MRI study. *Eur Spine J*. 1999;8(5):396-401. doi:10.1007/s005860050193

21. Siepe CJ, Zelenkov P, Sauri-Barraza JC, et al. The fate of facet joint and adjacent level disc degeneration following total lumbar disc replacement: a prospective clinical, x-ray, and magnetic resonance imaging investigation. *Spine*. 2010;35(22):1991-2003. doi:10.1097/BRS.0b013e3181d6f878

22. Lim CH, Jee WH, Son BC, Kim DH, Ha KY, Park CK. Discogenic lumbar pain: association with MR imaging and CT discography. *Eur J Radiol*. 2005;54(3):431-437. doi:10.1016/j.ejrad.2004.05.014

23. Eubanks JD, Lee MJ, Cassinelli E, Ahn NU. Prevalence of lumbar facet arthrosis and its relationship to age, sex, and race: an anatomic study of cadaveric specimens. *Spine*. 2007;32(19):2058-2062. doi:10.1097/BRS.0b013e318145a3a9

24. Li J, Muehleman C, Abe Y, Masuda K. Prevalence of facet joint degeneration in association with intervertebral joint degeneration in a sample of organ donors: facet joint degeneration. *J Orthop Res*. 2011;29(8):1267-1274. doi:10.1002/jor.21387

25. Hicks GE, Morone N, Weiner DK. Degenerative lumbar disc and facet disease in older adults: prevalence and clinical correlates. *Spine*. 2009;34(12):1301-1306. doi:10.1097/BRS.0b013e3181a18263

26. Suri P, Miyakoshi A, Hunter DJ, et al. Does lumbar spinal degeneration begin with the anterior structures? A study of the observed epidemiology in a community-based population. *BMC Musculoskelet Disord*. 2011;12(1):202. doi:10.1186/1471-2474-12-202

27. Kim JS, Ahmadinia K, Li X, et al. Development of an experimental animal model for lower back pain by percutaneous injury-induced lumbar facet joint osteoarthritis. *J Cell Physiol*. 2015;230(11):2837-2847. doi:10.1002/jcp.25015

28. Ni S, Cao Y, Liao S, et al. Unilateral osteotomy of lumbar facet joint induces a mouse model of lumbar facet joint osteoarthritis. *Spine*. 2019;44(16):E930-E938. doi:10.1097/BRS.0000000000003023

29. Yeh TT, Wen ZH, Lee HS, et al. Intra-articular injection of collagenase induced experimental osteoarthritis of the lumbar facet joint in rats. *Eur Spine J*. 2008;17(5):734-742. doi:10.1007/s00586-008-0594-0

30. Kim JS, Kroin JS, Buvanendran A, et al. Characterization of a new animal model for evaluation and treatment of back pain due to lumbar facet joint osteoarthritis. *Arthritis Rheum*. 2011;63(10):2966-2973. doi:10.1002/art.30487

31. Gong K, Shao W, Chen H, Wang Z, Luo ZJ. Rat model of lumbar facet joint osteoarthritis associated with facet-mediated mechanical hyperalgesia induced by intra-articular injection of monosodium iodoacetate. *J Formos Med Assoc*. 2011;110(3):145-152. doi:10.1016/S0929-6646(11)60024-7

32. Shuang F, Hou SX, Zhu JL, et al. Establishment of a rat model of lumbar facet joint osteoarthritis using intraarticular injection of urinary plasminogen activator. *Sci Rep*. 2015;5(1):9828. doi:10.1038/srep09828

33. Lotz JC, Colliou OK, Chin JR, Duncan NA, Liebenberg E. Compression-induced degeneration of the intervertebral disc: an in vivo mouse model and finite-element study. *Spine*. 1998;23(23):2493-2506. doi:10.1097/00007632-199812010-00004

34. Lotz JC, Chin JR. Intervertebral disc cell death is dependent on the magnitude and duration of spinal loading. *Spine*. 2000;25(12):1477-1483.

35. Stokes IAF, Iatridis JC. Mechanical conditions that accelerate intervertebral disc degeneration: overload versus immobilization. *Spine*. 2004;29(23):2724-2732. doi:10.1097/01.brs.0000146049.52152.da

36. Henry JL, Yashpal K, Vernon H, Kim J, Im HJ. Lumbar facet joint compressive injury induces lasting changes in local structure, nociceptive scores, and inflammatory mediators in a novel rat model. *Pain Res Treat*. 2012;2012:1-11. doi:10.1155/2012/127636

37. Lu Y, Pei S, Hou S. Development of a novel rat model of lumbar facet joint osteoarthritis induced by persistent compressive injury. *Exp Ther Med*. 2020;20:3740-3748. doi:10.3892/etm.2020.9117

38. Moore RJ, Osti OL, Vernon-Roberts B. Osteoarthosis of the facet joints resulting from anular rim lesions in sheep lumbar discs. *Spine*. 1999;24(6):519-525.

39. Wang T, Pelletier MH, Christou C, Oliver R, Mobbs RJ, Walsh WR. A novel in vivo large animal model of lumbar spinal joint degeneration. *Spine J*. 2018;18(10):1896-1909. doi:10.1016/j.spinee.2018.05.022

40. Rutges JPHJ, Jagt van der OP, Oner FC, et al. Micro-CT quantification of subchondral endplate changes in intervertebral disc degeneration. *Osteoarthr Cartil*. 2011;19(1):89-95. doi:10.1016/j.joca.2010.09.010

41. Wang Y, Battié MC, Boyd SK, Videman T. The osseous endplates in lumbar vertebrae: thickness, bone mineral density and their associations with age and disk degeneration. *Bone*. 2011;48(4):804-809. doi:10.1016/j.bone.2010.12.005

42. Rade M, Määttä JH, Freidin MB, Airaksinen O, Karppinen J, Williams FMK. Vertebral endplate defect as initiating factor in intervertebral disc degeneration: strong association between endplate defect and disc degeneration in the general population. *Spine*. 2018;43(6):412-419. doi:10.1097/BRS.0000000000002352

43. Zehra U, Cheung JPY, Bow C, Lu W, Samartzis D. Multidimensional vertebral endplate defects are associated with disc degeneration, modic changes, facet joint abnormalities, and pain. *J Orthop Res*. 2019;37(5):1080-1089. doi:10.1002/jor.24195

44. Benneker LM, Heini PF, Alini M, Anderson SE, Ito K. 2004 Young Investigator Award Winner: vertebral endplate marrow contact channel occlusions and intervertebral disc degeneration. *Spine*. 2005;30(2):167-173. doi:10.1097/01.brs.0000150833.93248.09

45. Kang R, Li H, Ringgaard S, et al. Interference in the endplate nutritional pathway causes intervertebral disc degeneration in an immature porcine model. *Int Orthop*. 2014;38(5):1011-1017. doi:10.1007/s00264-014-2319-9

46. Zhao H, Ni CF, Huang J, et al. Effects of bone cement on intervertebral disc degeneration. *Exp Ther Med*. 2014;7(4):963-969. doi:10.3892/etm.2014.1531

47. Yin S, Du H, Zhao W, et al. Inhibition of both endplate nutritional pathways results in intervertebral disc degeneration in a goat model. *J Orthop Surg*. 2019;14(1):138. doi:10.1186/s13018-019-1188-8

48. Ashinsky BG, Bonnevie ED, Mandalapu SA, et al. Intervertebral disc degeneration is associated with aberrant endplate remodeling and reduced small molecule transport. *J Bone Miner Res*. 2020;35(8):1572-1581. doi:10.1002/jbmr.4009

49. Hee HT, Chuah YJ, Tan BHM, Setiobudi T, Wong HK. Vascularization and morphological changes of the endplate after axial compression and distraction of the intervertebral disc. *Spine*. 2011;36(7):505-511. doi:10.1097/BRS.0b013e3181d32410

50. Jin L, Balian G, Li XJ. Animal models for disc degeneration—an update. *Histol Histopathol*. 2018;6:543-554. doi:10.14670/HH-11-910

51. Gullbrand SE, Ashinsky BG, Lai A, et al. Development of a standardized histopathology scoring system for intervertebral disc degeneration and regeneration in rabbit models—an initiative of the ORS spine section. *JOR Spine*. 2021;4(2):e1147. doi:10.1002/jsp2.1147

52. Beckstein JC, Sen S, Schaer TP, Vresilovic EJ, Elliott DM. Comparison of animal discs used in disc research to human lumbar disc: axial compression mechanics and glycosaminoglycan content. *Spine*. 2008;33(6):E166-E173. doi:10.1097/BRS.0b013e318166e001

53. Ashinsky BG, Gullbrand SE, Bonnevie ED, et al. Multiscale and multimodal structure–function analysis of intervertebral disc degeneration in a rabbit model. *Osteoarthr Cartil*. 2019;27(12):1860-1869. doi:10.1016/j.joca.2019.07.016

54. Sobajima S, Kompel JF, Kim JS, et al. A slowly progressive and reproducible animal model of intervertebral disc degeneration characterized by MRI, x-ray, and histology. *Spine*. 2005;30(1):15-24. doi:10.1097/01.brs.0000148048.15348.9b

55. Vadalà G, Sowa G, Hubert M, Gilbertson LG, Denaro V, Kang JD. Mesenchymal stem cells injection in degenerated intervertebral disc: cell leakage may induce osteophyte formation. *J Tissue Eng Regen Med*. 2012;6(5):348-355. doi:10.1002/term.433

56. Hoogendoorn RJW, Helder MN, Kroeze RJ, Bank RA, Smit TH, Wuisman PIJM. Reproducible long-term disc degeneration in a large animal model. *Spine*. 2008;33(9):949-954. doi:10.1097/BRS.0b013e31816c90f0

57. Bernick S, Cailliet R. Vertebral end-plate changes with aging of human vertebrae. *Spine*. 1982;7(2):97-102.

58. Haefeli M, Kalberer F, Saegesser D, Nerlich AG, Boos N, Paesold G. The course of macroscopic degeneration in the human lumbar intervertebral disc. *Spine*. 2006;31(14):1522-1531. doi:10.1097/01.brs.0000222032.52336.8e

59. de Bruin F, ter Horst S, Bloem HL, et al. Prevalence of degenerative changes of the spine on magnetic resonance images and radiographs in patients aged 16–45 years with chronic back pain of short duration in the Spondyloarthritis Caught Early (SPACE) cohort. *Rheumatology*. 2016;55(1):56-65. doi:10.1093/rheumatology/kev283

60. Martin JT, Gorth DJ, Beattie EE, Harfe BD, Smith LJ, Elliott DM. Needle puncture injury causes acute and long-term mechanical deficiency in a mouse model of intervertebral disc degeneration. *J Orthop Res*. 2013;31(8):1276-1282. doi:10.1002/jor.22355

61. Martin JT, Collins CM, Ikuta K, et al. Population average T_2 MRI maps reveal quantitative regional transformations in the degenerating rabbit intervertebral disc that vary by lumbar level. *J Orthop Res*. 2015;33(1):140-148. doi:10.1002/jor.22737

62. Gullbrand SE, Ashinsky BG, Martin JT, et al. Correlations between quantitative T_2 and $T_1 \rho$ MRI, mechanical properties and biochemical composition in a rabbit lumbar intervertebral disc degeneration model: T_2 and $T_1 \rho$ MRI correlations. *J Orthop Res*. 2016;34(8):1382-1388. doi:10.1002/jor.23269

63. Meloni GR, Fisher MB, Stoeckl BD, Dodge GR, Mauck RL. Biphasic finite element modeling reconciles mechanical properties of tissue-engineered cartilage constructs across testing platforms. *Tissue Eng Part A*. 2017;23(13–14):663-674. doi:10.1089/ten.tea.2016.0191

64. Gupta S, Xiao R, Fainor M, Mauck RL, Smith HE, Gullbrand SE. Level dependent alterations in human facet cartilage mechanics and bone morphometry with spine degeneration. *J Orthop Res*. 2022;41:674-683. doi:10.1002/jor.25407

65. Moore AC, DeLucca JF, Elliott DM, Burris DL. Quantifying cartilage contact modulus, tension modulus, and permeability with Hertzian biphasic creep. *J Tribol*. 2016;138(4):041405. doi:10.1115/1.4032917

66. Laverty S, Girard CA, Williams JM, Hunziker EB, Pritzker KPH. The OARSI histopathology initiative—recommendations for histological assessments of osteoarthritis in the rabbit. *Osteoarthr Cartil*. 2010;18:S53-S65. doi:10.1016/j.joca.2010.05.029

67. Elliott DM, Yerramalli CS, Beckstein JC, Boxberger JI, Johannessen W, Vresilovic EJ. The effect of relative needle diameter in puncture and sham injection animal models of degeneration. *Spine*. 2008;33(6):588-596. doi:10.1097/BRS.0b013e318166e0a2

68. Masuda K, Aota Y, Muehleman C, et al. A novel rabbit model of mild, reproducible disc degeneration by an anulus needle puncture: correlation between the degree of disc injury and radiological and histological appearances of disc degeneration. *Spine*. 2005;30(1):5-14. doi:10.1097/01.brs.0000148152.04401.20

69. Luo TD, Marquez-Lara A, Zabarsky ZK, et al. A percutaneous, minimally invasive annulus fibrosus needle puncture model of intervertebral disc degeneration in rabbits. *J Orthop Surg*. 2018;26(3):230949901879271. doi:10.1177/2309499018792715

70. Wong J, Sampson SL, Bell-Briones H, et al. Nutrient supply and nucleus pulposus cell function: effects of the transport properties of the cartilage endplate and potential implications for intradiscal biologic therapy. *Osteoarthr Cartil*. 2019;27(6):956-964. doi:10.1016/j.joca.2019.01.013

71. Fine N, Lively S, Séguin CA, Perruccio AV, Kapoor M, Rampersaud R. Intervertebral disc degeneration and osteoarthritis: a common

molecular disease spectrum. *Nat Rev Rheumatol*. 2023;19(3):136-152. doi:10.1038/s41584-022-00888-z

72. Donell S. Subchondral bone remodelling in osteoarthritis. *EFORT Open Rev*. 2019;4(6):221-229. doi:10.1302/2058-5241.4.180102

73. Jaumard NV, Welch WC, Winkelstein BA. Spinal facet joint biomechanics and mechanotransduction in normal, injury and degenerative conditions. *J Biomech Eng*. 2011;133(7):071010. doi:10.1115/1.4004493

74. Armstrong CG, Mow VC. Variations in the intrinsic mechanical properties of human articular cartilage with age, degeneration, and water content. *J Bone Joint Surg Am*. 1982;64(1):88-94. doi:10.2106/00004623-198264010-00013

75. Bae WC, Temple MM, Amiel D, Coutts RD, Niederauer GG, Sah RL. Indentation testing of human cartilage: sensitivity to articular surface degeneration. *Arthritis Rheum*. 2003;48(12):3382-3394. doi:10.1002/art.11347

76. Temple-Wong MM, Bae WC, Chen MQ, et al. Biomechanical, structural, and biochemical indices of degenerative and osteoarthritic deterioration of adult human articular cartilage of the femoral condyle. *Osteoarthr Cartil*. 2009;17(11):1469-1476. doi:10.1016/j.joca.2009.04.017

77. Temple MM, Bae WC, Chen MQ, et al. Age- and site-associated biomechanical weakening of human articular cartilage of the femoral condyle. *Osteoarthr Cartil*. 2007;15(9):1042-1052. doi:10.1016/j.joca.2007.03.005

78. Graham BT, Wright AD, Burris DL, Axe MJ, Raisis LW, Price C. Quantification of solute diffusivity in osteoarthritic human femoral cartilage using correlation spectroscopy. *J Orthop Res*. 2018;36(12):3256-3267. doi:10.1002/jor.24138

79. Ebrahimi M, Ojanen S, Mohammadi A, et al. Elastic, viscoelastic, and fibril-reinforced poroelastic material properties of healthy and osteoarthritic human tibial cartilage. *Ann Biomed Eng*. 2019;47(4):953-966. doi:10.1007/s10439-019-02213-4

80. Mäkelä JTA, Han SK, Herzog W, Korhonen RK. Very early osteoarthritis changes sensitively fluid flow properties of articular cartilage. *J Biomech*. 2015;48(12):3369-3376. doi:10.1016/j.jbiomech.2015.06.010

81. Ayral X, Pickering EH, Woodworth TG, Mackillop N, Dougados M. Synovitis: a potential predictive factor of structural progression of medial tibiofemoral knee osteoarthritis—results of a 1 year longitudinal arthroscopic study in 422 patients. *Osteoarthr Cartil*. 2005;13(5):361-367. doi:10.1016/j.joca.2005.01.005

82. Hügle T, Geurts J. What drives osteoarthritis?—synovial *versus* subchondral bone pathology. *Rheumatology*. 2016;56(9):1461-1471. doi:10.1093/rheumatology/kew389

83. Loeser RF. Molecular mechanisms of cartilage destruction: mechanics, inflammatory mediators, and aging collide. *Arthitis Rheum*. 2007;54(5):1357-1360.

84. Dunlop R, Adams M, Hutton W. Disc space narrowing and the lumbar facet joints. *J Bone Joint Surg Br*. 1984;66-B(5):706-710. doi:10.1302/0301-620X.66B5.6501365

85. An HS, Masuda K, Inoue N. Intervertebral disc degeneration: biological biomechanical factors. *J Orthop Sci*. 2006;11(5):541-552. doi:10.1007/s00776-006-1055-4

86. Li W, Wang S, Xia Q, et al. Lumbar facet joint motion in patients with degenerative disc disease at affected and adjacent levels: an in vivo biomechanical study. *Spine*. 2011;36(10):E629-E637. doi:10.1097/BRS.0b013e3181faaef7

87. Liu YK, Goel VK, Dejong A, Njus G, Nishiyama K, Buckwalter J. Torsional fatigue of the lumbar intervertebral joints. *Spine*. 1985;10(10):894-900.

88. Malfair D, Beall DP. Imaging the degenerative diseases of the lumbar spine. *Magn Reson Imaging Clin N Am*. 2007;15(2):221-238. doi:10.1016/j.mric.2007.04.001

89. Parker DA, Beatty KT, Giuffre B, Scholes CJ, Coolican MRJ. Articular cartilage changes in patients with osteoarthritis after osteotomy. *Am J Sports Med*. 2011;39(5):1039-1045. doi:10.1177/0363546510392702

90. Trinh TQ, Harris JD, Siston RA, Flanigan DC. Improved outcomes with combined autologous chondrocyte implantation and patellofemoral osteotomy versus isolated autologous chondrocyte implantation. *Arthroscopy*. 2013;29(3):566-574. doi:10.1016/j.arthro.2012.10.008

91. Flouzat-Lachaniette CH, Roubineau F, Heyberger C, Bouthors C. Distraction to treat knee osteoarthritis. *Joint Bone Spine*. 2017;84(2):141-144. doi:10.1016/j.jbspin.2016.03.004

92. Karamchedu NP, Murray MM, Sieker JT, et al. Bridge-enhanced anterior cruciate ligament repair leads to greater limb asymmetry and less cartilage damage than untreated ACL transection or ACL reconstruction in the porcine model. *Am J Sports Med*. 2021;49(3):667-674. doi:10.1177/0363546521989265

93. Beresford ZM, Kendall RW, Willick SE. Lumbar facet syndromes. *Curr Sports Med Rep*. 2010;9(1):50-56. doi:10.1249/JSR.0b013e3181caba05

94. Chen Y, Sun Y, Pan X, Ho K, Li G. Joint distraction attenuates osteoarthritis by reducing secondary inflammation, cartilage degeneration and subchondral bone aberrant change. *Osteoarthr Cartil*. 2015;23(10):1728-1735. doi:10.1016/j.joca.2015.05.018

95. Sun ZB, Peng H. Experimental study on the prevention of posttraumatic osteoarthritis in the rabbit knee using a hinged external fixator in combination with exercises. *J Invest Surg*. 2019;32(6):552-559. doi:10.1080/08941939.2018.1543483

96. Wiegant K, Intema F, Roermund PM, et al. Evidence of cartilage repair by joint distraction in a canine model of osteoarthritis. *Arthritis Rheumatol*. 2015;67(2):465-474. doi:10.1002/art.38906

97. Pye SR, Reid DM, Lunt M, Adams JE, Silman AJ, O'Neill TW. Lumbar disc degeneration: association between osteophytes, end-plate sclerosis and disc space narrowing. *Ann Rheum Dis*. 2007;66(3):330-333. doi:10.1136/ard.2006.052522

98. Kumaresan S, Yoganandan N, Pintar FA, Maiman DJ, Goel VK. Contribution of disc degeneration to osteophyte formation in the cervical spine: a biomechanical investigation. *J Orthop Res*. 2001;19(5):977-984. doi:10.1016/S0736-0266(01)00010-9

99. Iatridis JC, Mente PL, Stokes IAF, Aronsson DD, Alini M. Compression-induced changes in intervertebral disc properties in a rat tail model. *Spine*. 1999;24(10):996-1002. doi:10.1097/00007632-199905150-00013

100. Kroeber MW, Unglaub F, Wang H, et al. New in vivo animal model to create intervertebral disc degeneration and to investigate the effects of therapeutic strategies to stimulate disc regeneration. *Spine*. 2002;27(23):2684-2690. doi:10.1097/00007632-200212010-00007

101. Yang K, Song Z, Jia D, et al. Comparisons between needle puncture and chondroitinase ABC to induce intervertebral disc degeneration in rabbits. *Eur Spine J*. 2022;31(10):2788-2800. doi:10.1007/s00586-022-07287-8

102. Peeters M, Detiger SEL, Karfeld-Sulzer LS, et al. BMP-2 and BMP-2/7 heterodimers conjugated to a fibrin/hyaluronic acid hydrogel in a large animal model of mild intervertebral disc degeneration. *BioResearch Open Access*. 2015;4(1):398-406. doi:10.1089/biores.2015.0025

103. Cui H, Du X, Liu C, et al. Visfatin promotes intervertebral disc degeneration by inducing IL-6 expression through the ERK/-JNK/p38 signalling pathways. *Adipocyte*. 2021;10(1):201-215. doi:10.1080/21623945.2021.1910155

104. Kim KS, Yoon ST, Li J, Park JS, Hutton WC. Disc degeneration in the rabbit: a biochemical and radiological comparison between four disc injury models. *Spine*. 2005;30(1):33-37. doi:10.1097/01.brs.0000149191.02304.9b

105. Peng B, Li Y. Concerns about cell therapy for intervertebral disc degeneration. *npj Regen Med*. 2022;7(1):46. doi:10.1038/s41536-022-00245-4

106. Tong W, Lu Z, Qin L, et al. Cell therapy for the degenerating intervertebral disc. *Transl Res*. 2017;*181*:49-58. doi:10.1016/j.trsl.2016.11.008

SUPPORTING INFORMATION

Additional supporting information can be found online in the Supporting Information section at the end of this article.